

1072 10 10 5

**NASA TECHNICAL  
MEMORANDUM**

NASA TM X-68004

NASA TM X-68004

**CASE FILE  
COPY**

PARTICLE-HOLE STATES IN  $^{120}\text{Sn}$

by Regis F. Leonard  
Lewis Research Center  
Cleveland, Ohio

TECHNICAL PAPER proposed for presentation at  
American Physical Society Meeting  
San Francisco, California,  
January 31-February 3, 1972

# PARTICLE-HOLE STATES IN $^{120}\text{Sn}$

by Regis F. Leonard

Lewis Research Center

$^{120}\text{Sn}$  consists of a closed ( $Z = 50$ ) proton shell. Consequently, one should expect to see levels formed by the excitation of a single proton to the next higher shell. In tin such particle-hole states would be formed by coupling a  $g_{9/2}$ ,  $p_{1/2}$ ,  $p_{3/2}$ , or  $f_{5/2}$  hole to a  $d_{5/2}$ ,  $g_{7/2}$ ,  $d_{3/2}$ , or  $s_{1/2}$  particle, with each possible pairing resulting in a multiplet of states  $2J_{\min} + 1$  in number. The present experiment,  $^{121}\text{Sb}(d, ^3\text{He})^{120}\text{Sn}$ , should excite only those multiplets which are based on a  $d_{5/2}$  particle, since that is the dominant configuration of the  $^{121}\text{Sb}$  ground state. In addition ( $d, ^3\text{He}$ ) studies on the tin nuclei (ref. 1) indicate that no pickup from the  $f_{5/2}$  shell is observed in that reaction and that only one strong state is observed for each of the other L-value transfers. As a result one would expect to see just three multiplets in the present experiment, as illustrated in figure 1. These are the  $d_{5/2} \times (g_{9/2})^{-1}$  with a multiplicity of 6, the  $d_{5/2} \times (p_{1/2})^{-1}$  with a multiplicity of 2, and the  $d_{5/2} \times (p_{3/2})^{-1}$  with a multiplicity of 4. In addition one would expect the total strength and the energy centroid of each of these multiplets to be the same as that observed for the hole state in the  $^{120}\text{Sn}(d, ^3\text{He})^{119}\text{In}$  reaction at the same energy. Previous ( $^3\text{He}, d$ ) experiments (refs. 2 to 4) as well as a ( $t, \alpha$ ) experiment (ref. 5) have indicated the existence of such states in tin. The present work resolves a number of such individual levels and compares their strength and excitation energy with that observed in the  $^{120}\text{Sn}(d, ^3\text{He})$  reaction, which was also remeasured here.

The present work was carried out using the 45-MeV deuteron beam from the Berkeley 88-inch cyclotron. A schematic diagram of the scattering system is shown in figure 2. It is described in detail elsewhere (ref. 6). The arrangement consisted of momentum-analysis of the incident beam, isotopically enriched targets of antimony ( $0.15 \text{ mg/cm}^2$ ) and tin ( $0.40 \text{ mg/cm}^2$ ), solid-state E and  $\Delta E$  detectors, and

particle identification using standard Goulding-Landis circuitry. A typical energy spectrum from the  $^{121}\text{Sb}(d, {}^3\text{He})$  reaction is shown in figure 3. An overall energy resolution of 50 keV was obtained for most of the runs. This permitted observation of a number of individual particle-hole states, although clearly some are still unresolved. For example, the peaks at 3.89, 4.46, and 4.69 MeV appear not to be singlets. Excitation energies were determined for a total of 21 states and angular distributions between  $10^\circ$  and  $30^\circ$  were measured for 19 of these plus the ground state. In the  $^{120}\text{Sn}(d, {}^3\text{He})$  reaction, angular distributions and spectroscopic factors were measured for the ground and first two excited states of indium. These results are in good agreement with reference 1.

DWBA calculations have been carried out to determine L-values and spectroscopic factors for each of the observed states. These were done using the computer code DWUCK (ref. 7) and the optical potentials shown in table I. The deuteron potential is taken from the work of Duelli et al. (ref. 8) and the  ${}^3\text{He}$  potential is from Gibson et al. (ref. 9).

Figure 4 shows angular distributions for four states which have  $L = 2$ . These are the ground state and states at 1.17, 2.21, and 2.41 MeV. Another weak  $L = 2$  state was seen at 2.10 MeV and is not shown here. The assignment  $L = 2$  for the 2.41 MeV state indicates that this is the positive parity state reported in reference 10, and not the  $3^-$  state seen in inelastic scattering (ref. 11).

The first observed particle-hole states occur at excitation energies of approximately 3 MeV. All of the states seen at energies higher than this have, as expected, angular momentum transfers of either 1 or 4. Angular distributions for the  $L = 4$  states are shown in figure 5 together with DWBA calculations. A total of six states was seen, just the number predicted by a particle-hole coupling model.

Figure 6 shows the angular distributions and calculations for six of the  $L = 1$  states which were observed. Three other weakly excited states at 3.89, 4.12, and 3.09 MeV are also best described as  $L = 1$ , which makes the number of  $L = 1$  states larger than predicted from particle-hole coupling.

A summary of this data is shown in figure 7, where spectroscopic strengths as well as excitation energies are given for each level. Also shown on this figure are the energy centroids for the  $L = 2$ ,  $L = 4$ , and  $L = 1$  levels. The location of the  $L = 4$  centroid indicates a residual particle-hole interaction of 660 keV, as compared with the value 600 keV reported by Biggerstaff et al. (ref. 3) for  $^{116}\text{Sn}$ .

Table II shows the same data and table III the summed spectroscopic strength for each of the angular momentum transfers. Also shown in table III are the strengths observed for  $g_{9/2}$ ,  $p_{1/2}$ , and  $p_{3/2}$  pickup from  $^{120}\text{Sn}$ , as well as the sum rule limit, assuming each shell to be completely filled. The strengths for the  $^{120}\text{Sn}$  experiment are taken from the work of Wieffenbach et al. (ref. 1) and Conjeaud et al. (ref. 12) as well as from an auxiliary experiment performed here.

It can be seen that for the  $L = 2$  pick up, approximately 70 percent of the expected strength is observed, although it is split into five different states. This splitting as well as the missing strength is probably due in part at least to configuration mixing in the ground state of antimony, which has been found in ( $^3\text{He}, d$ ) experiments to account for only 65 percent (ref. 13) of the  $d_{5/2}$  strength.

For the  $L = 4$  transitions at least six states are observed, however, these account for only about 25 percent of the strength expected from the sum rule, or about 40 percent that observed in pickup from tin. Qualitatively, the same thing appears to be true for the  $L = 1$  transitions, although  $p_{1/2}$  and  $p_{3/2}$  pickup cannot be distinguished. The total strength for all nine  $L = 1$  states is less than 2, as compared with the sum rule limit of 6 and the 3.4 observed in the tin experiments. Even considering the configuration mixing in the antimony ground state and the possible 25 percent experimental errors in the measured spectroscopic factors, it appears that a considerable amount of  $L = 4$  and  $L = 1$  strength is still unaccounted for. In addition, the energies of the  $L = 1$  states are slightly lower relative to the  $L = 4$  states than they are observed to be in indium. A large part of the breakdown of the simple model is probably due to mixing with levels which arise from the coupling of a hole to a particle in a higher shell ( $g_{7/2}$ ,  $d_{3/2}$ , or  $s_{1/2}$ ). These levels should appear at nearly the same excitation energies as the  $d_{5/2}$  states.

## REFERENCES

1. C. V. Wieffenbach and R. Tickle, Phys. Rev. 3C, 1668 (1971).
2. M. Conjeaud, S. Harar, and J. Picard, Phys. Letters 23, 104 (1966).
3. J. A. Biggerstaff, C. Bingham, P. D. Miller, J. Solomon, and K. K. Seth, Phys. Letters 25B, 273 (1967).
4. R. Shoup, J. D. Fox, and G. Vourvopoulos, Nucl. Phys. A135, 689 (1969).
5. M. L. Chatterjee, N. Cindro, M. Conjeaud, B. Fernandez, S. Harar, E. Thuriere, and M. Turk, Centre d'Etudes Nucléaires de Saclay Report CEA-N-1232 (1969), p. 42.
6. R. E. Hintz, F. B. Selph, W. S. Flood, B. G. Harvey, F. G. Resmini, and E. A. McClatchie, Nucl. Instr. Methods 72, 61 (1969).
7. P. D. Kunz, Private Communication.
8. B. Duelli, F. Hinterberger, G. Mairle, U. Schmidt-Rohr, P. Turek, and G. Wagner, Phys. Letters 23, 485 (1966).
9. E. F. Gibson, B. Ridley, J. J. Kraushaar, M. E. Rickey, and R. H. Bassel, Phys. Rev. 155, 1194 (1967).
10. E. J. Schneid, A. Prakash, and B. L. Cohen, Phys. Rev. 156, 1316 (1967).
11. O. Beer, A. ElBehay, P. Lopato, Y. Terrien, G. Vallois, and K. K. Seth, Private Communication.
12. M. Conjeaud, S. Harar, and E. Thuriere, Nucl. Phys. A129, 10 (1969).
13. M. Conjeaud, S. Harar, and Y. Cassagnou, Nucl. Phys. A117, 449 (1968).

TABLE I  
OPTICAL MODEL POTENTIALS

	REAL	IMAGINARY	SPIN-ORBIT
DEUTERON	V = 102.6 MeV R = 1.05 F a = 0.925 F	$W_D = 15.5$ MeV R = 1.27 F a = 0.801 F	$V_{SO} = 6.8$ MeV R = 1.05 F a = 0.925 F
HELIUM-3	V = 170.0 MeV R = 1.14 F a = 0.723 F	W = 17.4 MeV R = 1.60 F a = 0.81 F	----- ----- -----
BOUND STATE	R = 1.25 F a = 0.65 F	----- -----	$\lambda = 25$ -----

CS-61841

TABLE II  
SPECTROSCOPIC STRENGTHS FOR L = 1 TRANSITIONS,  
STRENGTHS ARE SHOWN BASED ON BOTH  $p_{1/2}$  &  $p_{3/2}$  PICKUP

E*, MeV	L	S	E*, MeV	L	S
0	2	0.47	4.12	1	0.099, 0.083
1.17	2	.19	4.23	4	0.65
1.93	--	-----	4.37	1	.39, 0.32
2.10	2	.01	4.46	1	.49, 0.39
2.21	2	.04	4.58	--	-----
2.41	2	.04	4.69	1	.34, 0.27
3.09	1	0.020, 0.016	4.77	4	.74
3.64	4	.094	4.92	1	.23, 0.19
3.75	4	.11	5.09	1	.24, 0.20
3.89	1	.078, 0.067	5.16	1	.26, 0.21
4.00	4	.53	5.23	4	.54

SUMMED SPECTROSCOPIC STRENGTHS COMPARED WITH OTHER EXPERIMENTAL RESULTS

SHELL	$^{121}\text{Sb}(d, ^3\text{He})$ PRESENT WORK	$^{120}\text{Sn}(d, ^3\text{He})$	$^{120}\text{Sn}(d, ^3\text{He})$	$^{120}\text{Sn}(d, ^3\text{He})$ PRESENT WORK	SUM RULE LIMIT
2d <sub>5/2</sub>	0.75	---	---	---	1.0
1g <sub>9/2</sub>	2.66	6.5	5.9	4.9	10.0
2p <sub>1/2</sub> 2p <sub>3/2</sub>	2.34, 1.75	3.4	3.3	3.6	~6.0

TABLE III

CS-61840

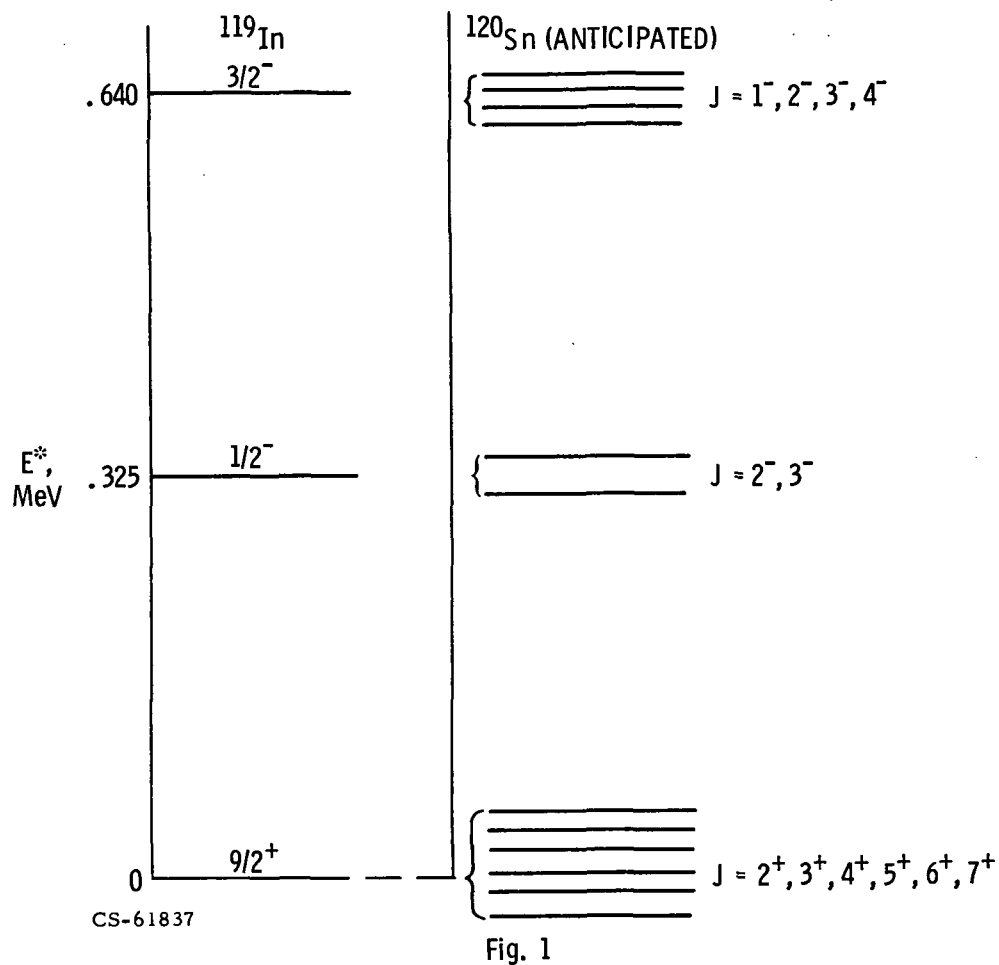


Fig. 1

### EXPERIMENTAL ARRANGEMENT

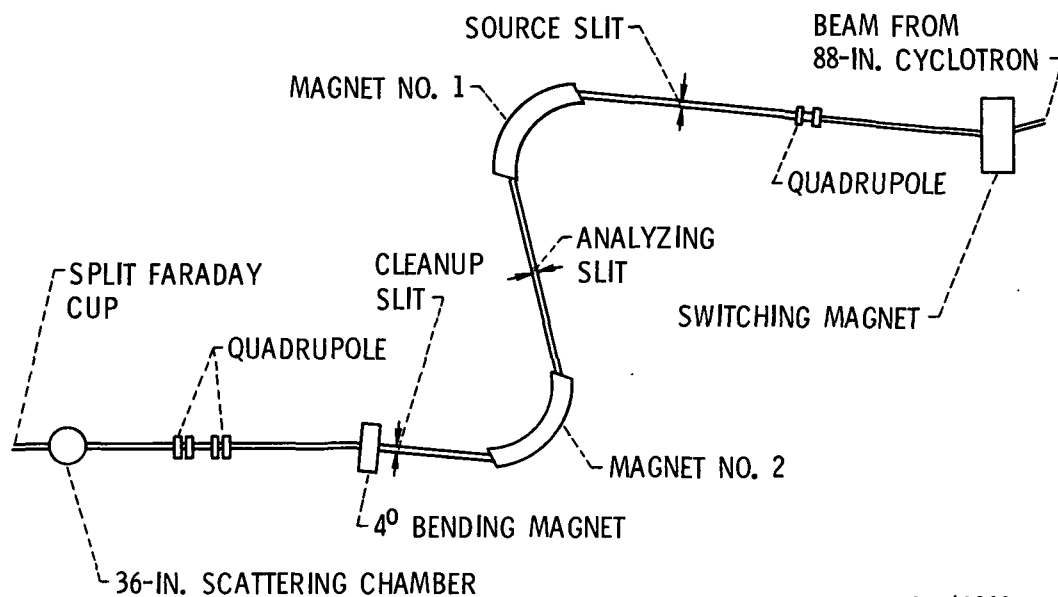
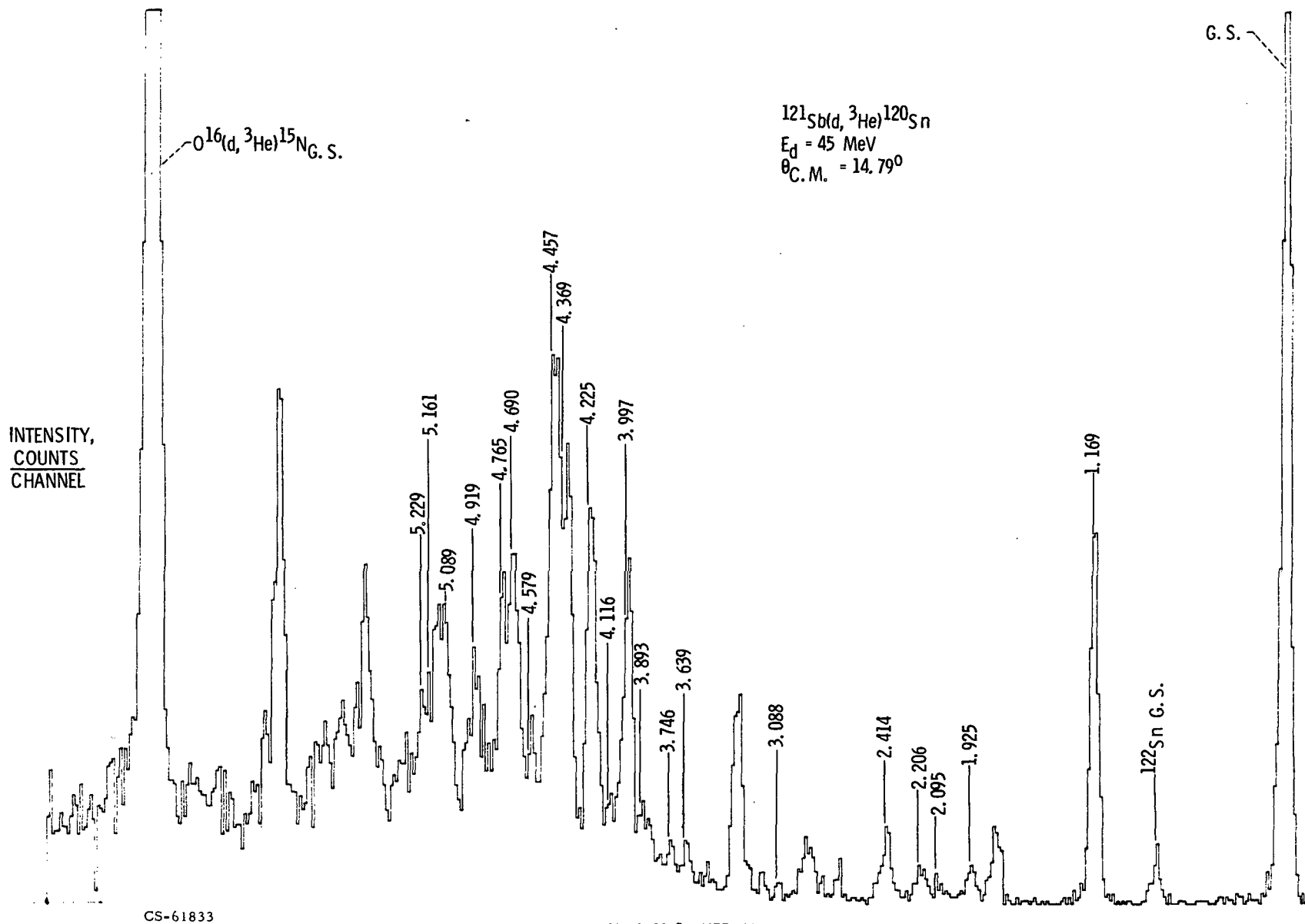


Fig. 2

CS-61838



HELIUM-3 ENERGY

Fig. 3



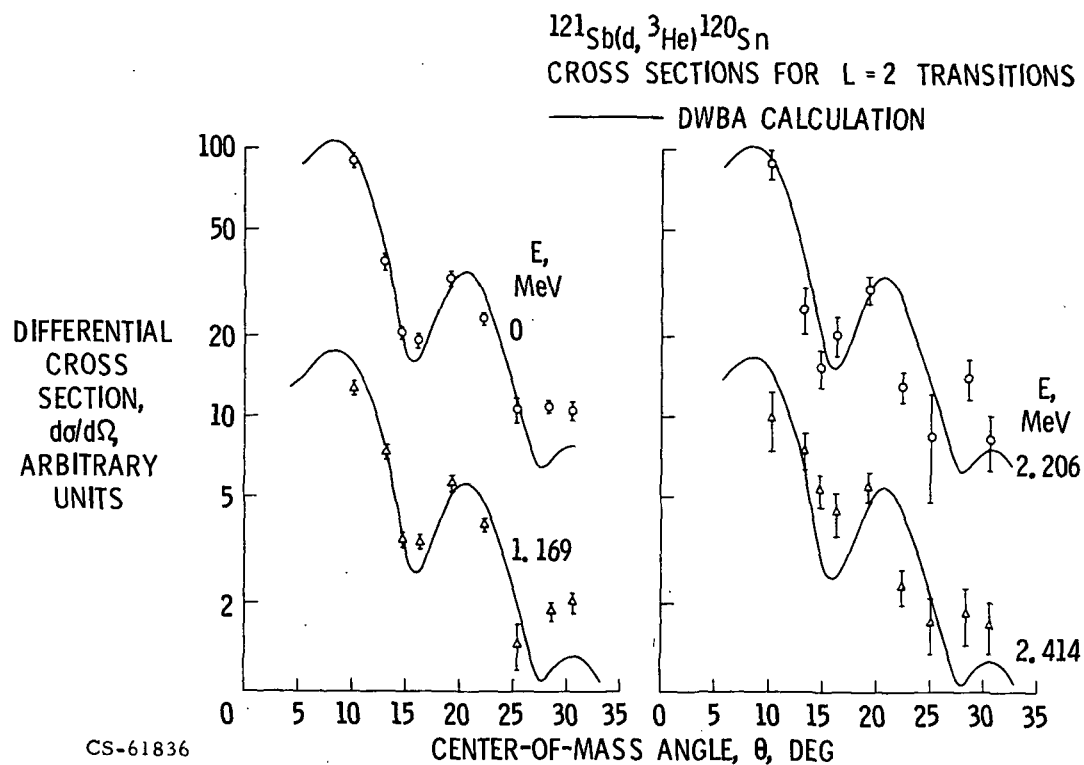


Fig. 4

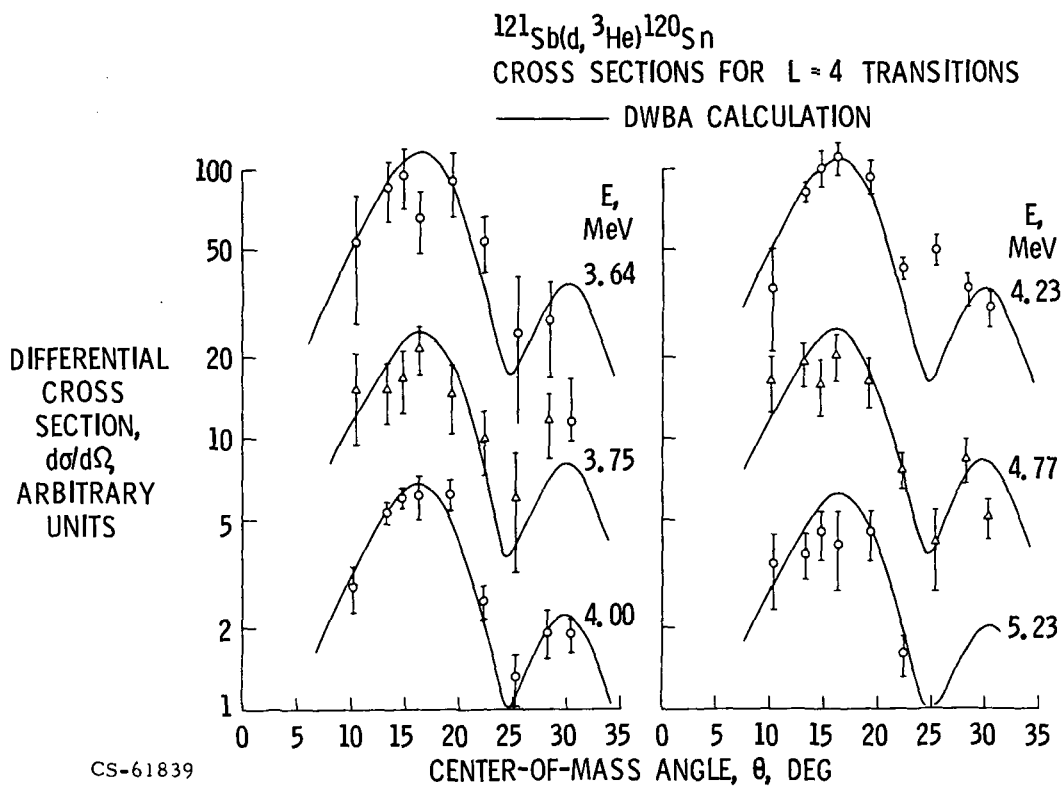


Fig. 5

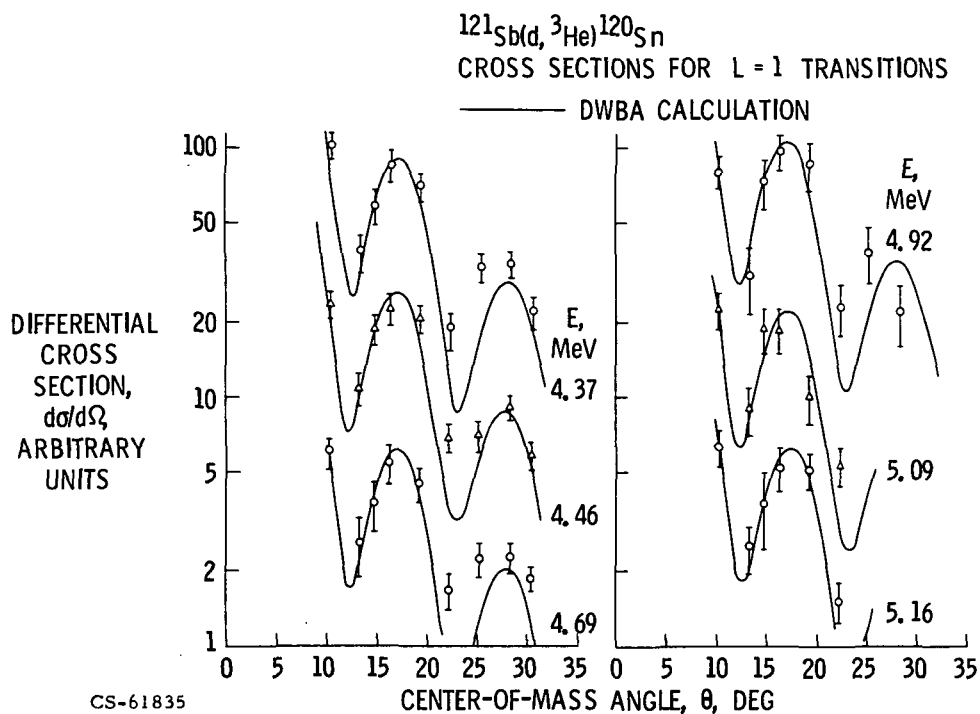


Fig. 6

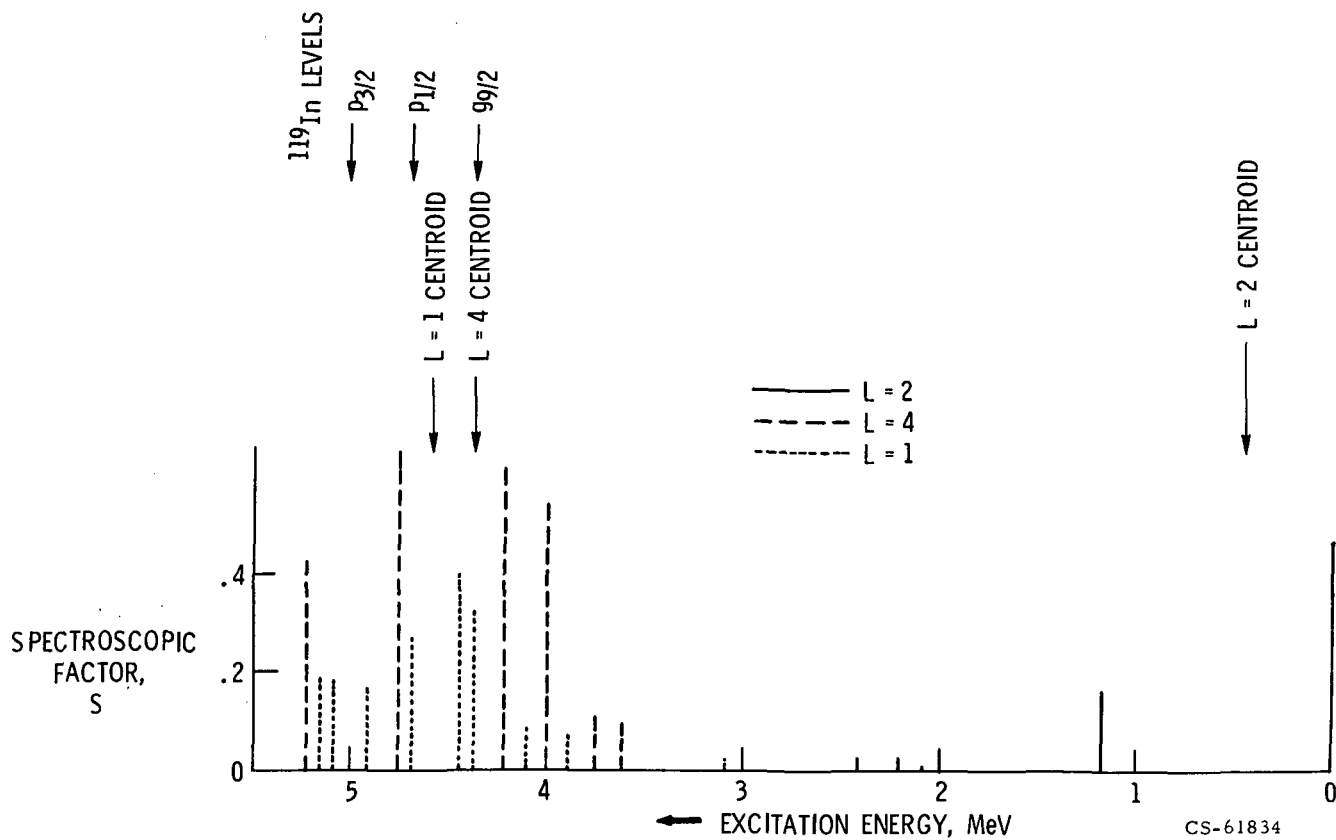


Fig. 7